

Cite this: DOI: 10.1039/xxxxxxxxxx

## Sub- $\mu$ L measurements of the thermal conductivity and heat capacity of liquids

Carlos López-Bueno,<sup>‡</sup> D. Bugallo,<sup>‡</sup> V. Leborán and F. Rivadulla\*

Received Date  
Accepted Date

DOI: 10.1039/xxxxxxxxxx

www.rsc.org/journalname

We present the analysis of the thermal conductivity,  $\kappa$ , and heat capacity,  $C_p$ , of a wide variety of liquids, covering organic molecular solvents, ionic liquids and water-polymer mixtures. These data were obtained from  $\approx 0.6 \mu\text{L}$  samples, using an experimental development based on the  $3\omega$  method, capable of the simultaneous measurement of  $\kappa$  and  $C_p$ . In spite of the different type and strength of interactions, expected in *a priori* so different systems, the ratio of  $\kappa$  to the sound velocity is approximately constant for all of them. This is the consequence of a similar atomic density for all these liquids, notwithstanding their different molecular structure. This was corroborated experimentally by the observation of a  $C_p/V \approx 1.89 \times 10^6 \text{ JK}^{-1} \text{ m}^{-3}$  ( $\approx 3R/2$  per atom), for all liquids studied in this work. Finally, the very small volume of sample required in this experimental method is an important advantage for the characterization of systems like nanofluids, in which having a large amount of dispersed phase is sometimes extremely challenging.

### 1 Introduction

The liquid state is the natural media where a large number of important physicochemical reactions occur, including many indispensable for life. The molecules of the solvent and solute exchange energy in different ways, determining the rate and even the feasibility of these reactions. The energy exchanged is stored in the different degrees of freedom of the molecules (at constant volume), which can be accessed through the macroscopic heat capacity,  $C_v$ . This thermodynamic magnitude, along with the thermal conductivity,  $\kappa$ , rules what are probably the most classical technological applications of liquids, *i.e.* their use as refrigerants and lubricants.<sup>1</sup> The low vapor pressure and chemical stability of ionic liquids, and the large variety of compositions available, make them attractive for the design of liquids with large ( $\kappa/C_p$ ) ratio.<sup>2–4</sup> A drawback of this strategy is the lack of a solid theoretical framework for the prediction of the thermodynamic properties of complex liquids from microscopic arguments. Another path followed in the last years is the use of nanofluids, dispersions of nanoparticles in a base liquid, whose thermal properties can be optimized by an adequate selection of the dispersed phase.<sup>5–11</sup> In this case, having the amount of disperse phase needed for sys-

tematic studies of  $\kappa$  and  $C_p$  (typically of several milliliters) can be challenging<sup>12,13</sup>. Optical methods can be applied to smaller volumes, but they are too complex and expensive for routine measurements.<sup>14,15</sup>

Here we present room temperature measurements of  $\kappa$  and  $C_p$  for a wide variety of liquids, including water-polymer mixtures, ionic liquids, and molecular solvents. These thermodynamic data were obtained from sample volumes  $\approx 0.6 \mu\text{L}$ , using an extension of the  $3\omega$  method.<sup>16</sup> The analysis of the data shows that the volumetric heat capacity is constant along a large variety of liquids, and equal to  $C_p/V \approx 1.87 \text{ JK}^{-1} \text{ m}^{-3}$ . As a consequence,  $\kappa$  shows linear dependence with the sound velocity,  $v_s$ , in all these liquids. Our results show that the volume available per atom determines the thermodynamic properties of the liquid, to a large extent. This can be helpful to predict the thermodynamic properties of several liquids, irrespective of their molecular structure.

### 2 Experimental

The  $3\omega$  method was originally developed by Cahill<sup>16</sup> to measure the thermal conductivity of solids: an AC current  $\propto \sin(\omega t)$  is flowed along a metallic line (used as a heater and sensor) deposited on the surface of the material under study. The power dissipated by Joule effect presents a sinusoidal component  $\propto I_0^2 \cos(2\omega t)$ , which produces a frequency dependent temperature oscillation of the metal,  $\Delta T_{2\omega}$ . Due to the temperature dependence of the resistance of the metallic line,  $dR/dT$ , the voltage measured along its length shows an oscillatory component  $\propto \sin(3\omega t)$  (see supporting information for a detailed de-

Centro de Investigación en Química Biológica e Materiais Moleculares (CIQUS), Universidade de Santiago de Compostela, 15782 Santiago de Compostela, Spain.; E-mail: frivadulla@usc.es

† Electronic Supplementary Information (ESI) available: Detailed derivation of the origin of the  $V_{3\omega}$  term from the solution of the heat equation, as well as the details for the calculation of  $\eta$  for obtaining accurate values of the heat capacity of the liquid. See DOI: 10.1039/b000000x/

‡ These authors contributed equally to this work.

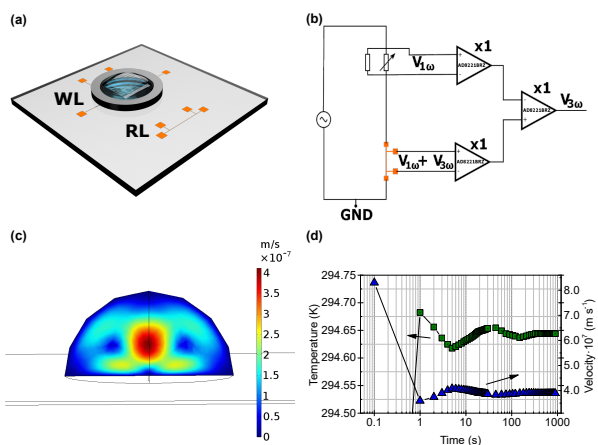


**Fig. 1** (a) Experimental setup for the measurement of the thermal conductivity and heat capacity of liquids. The working (WL) and reference lines (RL) are shown. (b) Scheme of the circuit used to eliminate the first harmonic component of the voltage, showing the configuration of the three differential amplifiers and the variable resistor in series with the Pt line. (c) Finite-element simulation of the convective flow velocity using liquid ethylene glycol. The simulation time and the heating power were set to 15 min and 5 mW. (d) Temperature distribution (squares) and flow velocity (triangles) at the center of the heater surface ( $T$  at  $t = 0$  s is 293.15 K) and at the point of maximum velocity, respectively. The steady state is reached after  $\approx 100$  s.

scription):

$$V_{3\omega} = \frac{I_0}{2} \left( \frac{dR}{dT} \right) \Delta T_{2\omega} \quad (1)$$

The magnitude of  $\Delta T_{2\omega}$  is related to the thermal diffusivity in the material, and can be obtained by solving the heat equation. For a sufficiently narrow metallic line, the mean temperature measured by this strip is given by<sup>16,17</sup>:

$$\Delta T = \frac{P}{\pi l \kappa} \left[ \frac{1}{2} \ln \left( \frac{\kappa}{b^2 \rho C} \right) - \frac{1}{2} \ln(2\omega) + \eta - \frac{i\pi}{4} \right] \quad (2)$$

where  $\kappa$ ,  $C$  and  $\rho$  are the thermal conductivity, heat capacity and density of the material under study (see supporting information for a detailed derivation of this equation). Given the relationship between  $V_{3\omega}$  and  $\Delta T_{2\omega}$  in equation (1),  $\kappa$  can be obtained from the slope of a  $V_{3\omega}$  vs.  $\ln(2\omega)$  plot.

On the other hand, if the metallic line is placed at the interface between two media with different  $\kappa$ ,  $V_{3\omega}(\omega)$  contains the information of the thermal properties of both of them. For the case of a solid-liquid interface, the result is an increase of the apparent thermal conductivity ( $\kappa_{s+l}$ ), from the sum of the thermal conductivities of the solid ( $\kappa_s$ ) and the liquid ( $\kappa_l$ )<sup>18</sup>. Equation (2) can be generalized to account for an interface of this type<sup>19,20</sup>:

$$\Delta T_{s+l} \approx \left[ \frac{P}{\pi l (\kappa_s + \kappa_l)} \mathcal{H}_l \left( \frac{b}{\delta_l} \right) \right] \left[ 1 + \frac{\kappa_s}{\kappa_s + \kappa_l} \left( \frac{\mathcal{H}_l(b/\delta_l)}{\mathcal{H}_s(b/\delta_s)} - 1 \right) \right]^{-1} \quad (3)$$

where  $\mathcal{H}_j(x) = -\ln(x) + \eta_j$ , and  $\delta$ :

$$\delta_j = \left( i \frac{2\omega(\rho C)_j}{\kappa_j} \right)^{-1/2} \quad (4)$$

Therefore, the thermal conductivity and heat capacity of the liquid could be obtained from a single  $V_{3\omega}(\omega)$  measurement, if the corresponding values of the solid substrate are previously obtained from an independent measurement (see supporting information for a detailed discussion).

The experimental setup developed in this paper is schematically shown in Figure 1a). Two identical lines of Cr(10 nm)/Pt(100 nm) ( $1 \text{ mm} \times 10 \mu\text{m}$ ) were deposited by standard photolithography and lift-off on top of a low thermal conductivity glass substrate (Corning® glass,  $\kappa \approx 0.9 \text{ Wm}^{-1}\text{K}^{-1}$ ). The length and width of the lines were properly optimized to increase the sensitivity of the device (see supporting information Figure S2).

On the other hand, Pt shows a large  $dR/dT$  coefficient, providing the level of resolution needed to discriminate the low values of  $\kappa$  characteristic of most liquids. One of the lines, the working line, is placed in contact with the liquid, while the other (separated  $\approx 3 \text{ mm}$ ) is used as a reference to obtain accurate values of  $\kappa$  of the glass substrate. In order to hold the liquid, a PELCO® silicon disk frame with a thickness of 200  $\mu\text{m}$  and square aperture of  $1 \times 1 \text{ mm}$  is secured on top of the working line. We place a volume of liquid in this receptacle  $\approx 0.6 \mu\text{L}$ .

An AC current from 56 Hz to 2.12 kHz was injected in the Pt lines using a Keithley 6221 AC current source. The frequency dependence of the  $3\omega$  voltage between the inner contacts of the Pt line was measured using a Stanford Research Systems SR830 lock-in amplifier. As the  $V_{1\omega}/V_{3\omega}$  ratio is typically  $10^3$ - $10^6$ , the  $1\omega$  voltage was suppressed with the circuit shown in Fig. 1b), prior to lock-in detection.

In order to study the effect of natural convection on the measurements, finite element simulations were performed with COMSOL®. The results are shown in Figure 1c) and d). The flow velocity and temperature distribution reach a steady state after 100 s. Therefore, a stabilization time protocol of several minutes was employed to eliminate any source of error of this type.

### 3 Results and Discussion

In Figure 2 we show a comparison between the frequency dependence of the  $V_{3\omega}$  for the reference line and the working Pt line in contact with 0.6  $\mu\text{L}$  of different liquids. The change in the slope due to different thermal conductivity can be perfectly appreciated.

The thermal conductivities at room temperature of the liquids studied in this work are shown in Table 1. Each value was measured at least three times with respect to the reference line. In order to validate the method and calibrate properly the setup, we selected for our measurements some liquids whose  $\kappa$  and  $C_p$  was previously measured by other experimental techniques, and are available in the literature. As can be seen from the results in Table 1, our values compare very satisfactorily with the results from the literature, with deviations within  $\approx 10 \%$  for most of them.<sup>21-28</sup> This demonstrates the accuracy of the method, using less than a microliter for each measurement.

The values of  $\kappa$  span from  $\approx 0.10 \text{ Wm}^{-1}\text{K}^{-1}$  for dichlorobenzene and some aprotic ionic liquids, to  $\approx 0.23 \text{ Wm}^{-1}\text{K}^{-1}$  for PEG or DMF. We have also measured solutions of different polymers in water, obtaining larger values of  $\kappa$ , up to  $\approx 0.4 \text{ Wm}^{-1}\text{K}^{-1}$

**Table 1** Density, molecular weight, thermal conductivity and heat capacity of the liquids studied in this work. The average values of the molecular weight,  $M^*$ , for the water-polymer mixture were calculated from the corresponding molar fractions of both phases. The error for each measurement is shown in brackets. The superscripts indicate the values of  $\kappa$  and  $C_p$  taken from the literature, for comparison (footnote).

Name	Chemical Formula	$\rho$ (g/cm <sup>3</sup> )	$M$ (g/mol)	$\kappa$ (W/mK)	$C_p$ (J/molK)
PVSA (25%wt.)	(C <sub>2</sub> H <sub>3</sub> NaO <sub>3</sub> S) <sub>n</sub>	1.267	22.93*	0.328(20)	62(4)
PDDA (20%wt.)	(C <sub>8</sub> H <sub>16</sub> NCl) <sub>n</sub>	1.04	21.90*	0.408(24)	46(5)
PAO 40	H(C <sub>10</sub> H <sub>20</sub> ) <sub>n</sub> H	0.8494	1400	0.150(14) <sup>a</sup>	3129(150)
TMPTO	C <sub>60</sub> H <sub>110</sub> O <sub>6</sub>	0.9184	927.534	0.150(14) <sup>b</sup>	1849(84) <sup>i</sup>
PEG 400	H(OCH <sub>2</sub> CH <sub>2</sub> ) <sub>n</sub> OH	1.128	400	0.232(10) <sup>c</sup>	732(32) <sup>j</sup>
DMF	HCON(CH <sub>3</sub> ) <sub>2</sub>	0.944	73.09	0.217(10) <sup>d</sup>	160(6) <sup>k</sup>
BzO	(C <sub>6</sub> H <sub>5</sub> CH <sub>2</sub> ) <sub>2</sub> O	1.043	198.26	0.128(9) <sup>e</sup>	307(32)
dClBz	C <sub>6</sub> H <sub>4</sub> Cl <sub>2</sub>	1.306	147.00	0.116(11) <sup>f</sup>	193(20)
[EMIM][NTF <sub>2</sub> ]	[C <sub>6</sub> H <sub>11</sub> N <sub>2</sub> ] <sup>+</sup> [N(SO <sub>2</sub> CF <sub>3</sub> ) <sub>2</sub> ] <sup>-</sup>	1.52	391.3	0.10(1) <sup>g</sup>	327(10)
[DEME][NTF <sub>2</sub> ]	[C <sub>8</sub> H <sub>20</sub> NO] <sup>+</sup> [N(SO <sub>2</sub> CF <sub>3</sub> ) <sub>2</sub> ] <sup>-</sup>	1.42	426.4	0.130(5)	569(34)
[BMIM][TFO]	[C <sub>8</sub> H <sub>15</sub> N <sub>2</sub> ] <sup>+</sup> [SO <sub>3</sub> CF <sub>3</sub> ] <sup>-</sup>	1.29	288.3	0.164(13)	375(10) <sup>l</sup>
[MOIM][PF <sub>6</sub> ]	[C <sub>12</sub> H <sub>23</sub> N <sub>2</sub> ] <sup>+</sup> [PF <sub>6</sub> ] <sup>-</sup>	1.24	340.29	0.147(13) <sup>h</sup>	514(27)

$\kappa$  (W/mK): a(Ref. 21)=0.164; b(Ref. 22)=0.16; c(Ref. 23)=0.265; d(Ref. 24)=0.198; e(Ref. 25)=0.139; f(Ref. 26)=0.122; g(Ref. 27)=0.12; h(Ref. 28)=0.147 —  $C_p$  (J/molK): i(Ref. 22)=1798; j(Ref. 29)=835.6; k(Ref. 30)=146.05; l(Ref. 32)=421.6.

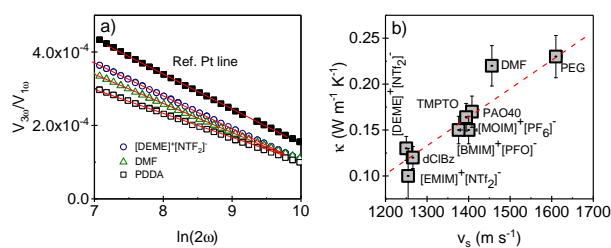


**Fig. 2** a) Frequency dependence of the  $3\omega$  voltage for the Pt reference line (solid squares), and for the working line in contact with different liquids (open symbols). b) Thermal conductivity vs. sound velocity for the pure liquids studied in this work.

( $\kappa(\text{H}_2\text{O})=0.60 \text{ Wm}^{-1}\text{K}^{-1}$ ).<sup>33</sup> From these data, a general trend of  $\kappa$  with the molecular mass, density or viscosity of the liquids is not evident.

The thermal conductivity represents the rate of energy transported along a given length of a system out of thermal equilibrium. From a kinetic argument we can therefore conclude that  $\kappa$  must be proportional to the energy stored locally by the system, and the velocity at which this energy is transported. A formal treatment of this idea using the Boltzmann transport equation in the relaxation time approximation, leads to the general relationship<sup>34</sup>:  $\kappa \propto C_v v \Lambda$ ; where  $C_v$ ,  $v$ , and  $\Lambda$  represent the volumetric heat capacity, the mean (isotropic) velocity of the heat-carrying excitations, and their mean-free path, respectively. If we ignore the molecular structure and think about the liquid as a collection of randomly distributed equivalent atoms, we can assign an average volume to each of them,  $V_a$  (Figure 3). In this picture, the volumetric heat capacity can be replaced by the product of a constant heat capacity per atom, and an atomic density,  $V_a^{-1}$ . The effect of interactions (such as H-bonds) on the heat capacity is taken into account through a reduction of  $V_a$ . Replacing  $v$  by the sound velocity,  $v_s$ , and  $\Lambda$  with a distance proportional to  $V_a^{1/3}$ , results in the following expression for the thermal conductivity of the liquid:

$$\kappa \propto \frac{k_B v_s}{V_a^{2/3}} \quad (5)$$

This resembles the equation obtained by Bridgman<sup>35</sup>, and Kincaid et al.<sup>36</sup>. The values of  $\kappa$  measured in this work for pure liquids are plotted in Figure 2 against  $v_s$ , taken from the literature<sup>31,32,37–42</sup>. The linearity of the representation shows that the average volume per atom remains approximately constant in all these liquids. Given that average atomic distances C-C, C-H, etc., are similar in different molecules, changes in  $V_a$  reflect variations in the intermolecular distance. In weakly interacting molecular liquids, like most measured in this work, the average intermolecular distance is not expected to vary much. Importantly, this trend is also obeyed in the case of the four aprotic ionic liquids, showing that their complex structure prevents strong anomalies in the available volume per atom even in the presence of Coulomb interactions. As mentioned before, liquids with strong interactions like H-bonding (water, protic ionic liquids, etc), should present a step-per proportionality of  $\kappa$  with  $v_s$ . Actually, the positive deviation of DMF from this line could be related to weak H-bonding between CH/CH<sub>3</sub> and C=O groups characteristic of this molecule.<sup>43,44</sup>

Recently, a phonon-like theory has been developed over the possibility of liquids to transmit shear waves of wavelengths close to interatomic separation.<sup>45–47</sup> One of the important derivations of this model is that the thermodynamic properties of liquids are governed by the interatomic separation, irrespective of disorder. This seems compatible with the interpretation of  $V_a$  as a fundamental length that governs the thermodynamic properties of the liquid, irrespective of its molecular structure.

As discussed before, the heat capacity of the liquid can be obtained from the intercept of the  $V_{3\omega}$  vs.  $\ln(2\omega)$  plot. This requires a careful measurement of the thermal conductivity and heat capacity of the substrate, and an accurate determination of the value of  $\eta$  in Eq. (2). For materials with low  $\kappa$ , the penetration depth of the thermal wave is small, and decreases further at high frequency. This situation departs from the limit where the approximations leading to equation (2) and (3) are justified. Therefore, we determined the experimental value of  $\eta$  (see supporting information) and fitted the real part of the  $V_{3\omega}$  to equation (3) to extract accurate values of  $C_p$ . The results are shown in Table 1; they compare very well with the values available in the literature<sup>29,30,32,48</sup>.

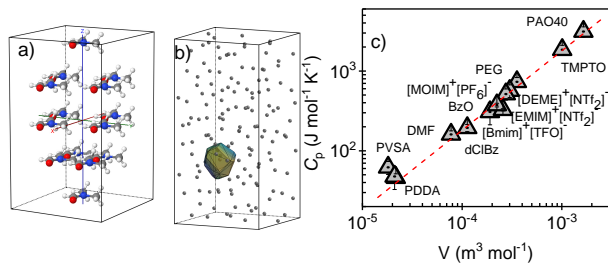


**Fig. 3** a) Molecular structure of liquid DMF. b) Random distribution of equivalent atoms, ignoring the molecular structure of DMF. The polygon encloses a volume  $V_a$ , representing an average volume per atom in this liquid. c) Heat capacity of the liquids versus the molar volume. The red line is a fitting to  $C_p(\text{JK}^{-1}\text{mol}^{-1}) = 6.5 + 1.89 \times 10^6 V(\text{m}^3\text{mol}^{-1})$ , see text.

The dependence of  $C_p$  with the molar volume is shown in Figure 3b). The linear dependence confirms our hypothesis about the constant volumetric heat capacity for the liquids studied in this work. Note moreover that the experimental method used in this work only rises the temperature of the liquid  $\approx 1$  K during the measurement. This, along with the small thermal expansion characteristic of most liquids makes the expansion work negligible, and  $C_p$  can be taken approximately equal to  $C_v$  in this case.

Paulechka et al.<sup>49,50</sup> proposed a relationship for the heat capacity of aprotic ionic liquids and their molar volume,  $C(\text{JK}^{-1}\text{mol}^{-1}) \approx 1.915 \times 10^6 V(\text{m}^3\text{mol}^{-1})$ , irrespective of the molecular structure. From the fitting of our data in Figure 3b),  $C_p(\text{JK}^{-1}\text{mol}^{-1}) \approx 1.89 \times 10^6 V(\text{m}^3\text{mol}^{-1})$ . Ignoring again the molecular structure of the liquid and normalizing this heat capacity to the number of atoms per mol,  $C \approx 1.44(0.25)R$ , for every liquid. Intramolecular vibrations are too high in energy to be excited at room temperature; therefore, this result is analogous to a kinetic contribution from every atom, like in monoatomic liquids. This shows that this relationship is probably general in the absence of strong intermolecular interactions, like for instance hydrogen bonds in water<sup>51</sup> and protic-ionic liquids.<sup>52</sup>

## 4 Conclusions

In summary, we analyzed the thermal conductivity and heat capacity of different liquids measured from 0.6  $\mu\text{L}$  samples. The results show a linear dependence of  $\kappa$  with the sound velocity, for a wide variety of liquids, including ionic and molecular liquids. This result is the consequence of a volumetric heat capacity which remains constant for all these liquids, in spite of their different molecular structure. The intermolecular distance determines the available volume per atom and governs the thermodynamic properties, playing the role of a fundamental distance in the liquid. Interestingly, the heat capacity in these complex liquids is  $\approx 3R/2$  per atom, like in monoatomic liquids. Finally, we want to remark the important advantages of the method proposed in this paper for the thermodynamic characterization of nanofluids, where large amounts of samples are difficult to obtain. It is also advantageous for measurements at cryogenic temperatures inside a cryostat, where the small size helps meeting the requirements of a good thermalization in a tight space.

## Conflicts of interest

There are no conflicts to declare.

## Acknowledgements

We acknowledge fruitful discussion with Dr. Kostya Trachenko from Queen Mary University of London. We also acknowledge Dr. Beatriz Pelaz and Dr. Josefa Fernández, from the University of Santiago de Compostela for providing some of the liquids studied in this paper. This work was supported by the Ministry of Science of Spain (Projects No. MAT2016-80762-R), the Consellería de Cultura, Educación e Ordenación Universitaria (ED431F 2016/008, and Centro singular de investigación de Galicia accreditation 2016-2019, ED431G/09), the European Regional Development Fund (ERDF).

## Notes and references

- 1 S. Gill and A. Rowntree, in *Liquid Lubricants for Spacecraft Applications*, ed. R. M. Mortier, M. F. Fox and S. T. Orszulik, Springer Netherlands, Dordrecht, 2010, pp. 375–387.
- 2 M.-D. Bermúdez, J. Jiménez, A.-E. an Sanes and F.-J. Carrión, *Molecules*, 2009, **14**, 2888–2908.
- 3 H. Zhao, *Chemical Engineering Communications*, 2006, **193**, 1660–1677.
- 4 M. E. Van Valkenburg, R. L. Vaughn, M. Williams and J. S. Wilkes, *Thermochimica Acta*, 2005, **425**, 181 – 188.
- 5 S. Angayarkanni and J. Philip, *Advances in Colloid and Interface Science*, 2015, **225**, 146 – 176.
- 6 S. Lee, S. Choi, S. Li and J. Eastman, *Journal of Heat Transfer*, 1999, **121**, 280–289.
- 7 X. Wang, X. Xu and S. Choi, *Journal of Thermophysics and Heat Transfer*, 1999, **13**, 474–480.
- 8 P. Keblinski, J. A. Eastman and D. G. Cahill, *Materials Today*, 2005, **8**, 36–44.
- 9 R. Prasher, P. Bhattacharya and P. E. Phelan, *Journal of Heat Transfer November*, 2005, **128**, 588.
- 10 X.-Q. Wang and A. S. Mujumdar, *International Journal of Thermal Sciences*, 2007, **46**, 1 – 19.
- 11 A. P. Nagvenkar, I. Perelshtein and A. Gedanken, *The Journal of Physical Chemistry C*, 2017, **121**, 26551–26557.
- 12 H. M. Rodert, *Journal of Research of the National Bureau of Standards*, 1981, **86**, year.
- 13 J. J. Healy, J. J. de Groot and J. Kestin, *Physica B+C*, 1976, **82**, 392 – 408.
- 14 J. Zhu, X. Wu, D. M. Lattery, W. Zheng and X. Wang, *Nanoscale and Microscale Thermophysical Engineering*, 2017, **21**, 177–198.
- 15 M. Hu, X. Wang, G. V. Hartland, V. Salgueiriño-Maceira and L. M. Liz-Marzán, *Chemical Physics Letters*, 2003, **372**, 767 – 772.
- 16 D. G. Cahill, *Review of Scientific Instruments*, 1990, **61**, 802–808.
- 17 J. Alvarez-Quintana and J. Rodríguez-Viejo, *Sensors and Actuators A: Physical*, 2008, **142**, 232 – 236.
- 18 D. G. Cahill and R. O. Pohl, *Phys. Rev. B*, 1987, **35**, 4067–4073.

- 19 F. Chen, J. Shulman, Y. Xue, C. W. Chu and G. S. Nolas, *Review of Scientific Instruments*, 2004, **75**, 4578–4584.
- 20 S. Gauthier, A. Giani and P. Combette, *Sensors and Actuators A: Physical*, 2013, **195**, 50 – 55.
- 21 E. R. Booser, *CRC Handbook of Lubrication and Tribology, Volume III: Monitoring, materials, synthetic lubricants, and applications*, CRC Press, 1993, vol. 3.
- 22 A. Pettersson, *Tribology International*, 2003, **36**, 815 – 820.
- 23 R. Rusconi, W. C. Williams, J. Buongiorno, R. Piazza and L.-W. Hu, *International Journal of Thermophysics*, 2007, **28**, 1131–1146.
- 24 M. B. Bryning, D. E. Milkie, M. F. Islam, J. M. Kikkawa and A. G. Yodh, *Applied Physics Letters*, 2005, **87**, 161909.
- 25 <https://comptox.epa.gov/dashboard/dsstoxdb/results?search=DTXSID5025819>.
- 26 <https://cameochemicals.noaa.gov/chris/DBO.pdf>.
- 27 A. P. Fröba, M. H. Rausch, K. Krzeminski, D. Assenbaum, P. Wasserscheid and A. Leipertz, *International Journal of Thermophysics*, 2010, **31**, 2059–2077.
- 28 D. Tomida, S. Kenmochi, T. Tsukada, K. Qiao and C. Yokoyama, *International Journal of Thermophysics*, 2007, **28**, 1147–1160.
- 29 <http://www.dynalene.com>.
- 30 J.-P. Grolier, G. Roux-Desgranges, M. Berkane, E. Jiménez and E. Wilhelm, *The Journal of Chemical Thermodynamics*, 1993, **25**, 41 – 50.
- 31 M. Dzida, M. Chorążewski, M. Geppert-Rybczyńska, E. Zorębski, M. Zorębski, M. Żarska and B. Czech, *Journal of Chemical & Engineering Data*, 2013, **58**, 1571–1576.
- 32 G. García-Miaja, J. Troncoso and L. Romani, *The Journal of Chemical Thermodynamics*, 2009, **41**, 161 – 166.
- 33 M. L. Ramires, C. A. Nieto de Castro, Y. Nagasaka, A. Nagashima, M. J. Assael and W. A. Wakeham, *Journal of Physical and Chemical Reference Data*, 1995, **24**, 1377–1381.
- 34 J. M. Ziman, *Electrons and Phonons. The Theory of Transport Phenomena in Solids*, Oxford University Press, London, UK, 1963.
- 35 P. W. Bridgman, *Proceedings of the American Academy of Arts and Sciences*, 1923, pp. 141–169.
- 36 J. F. Kincaid and H. Eyring, *The Journal of Chemical Physics*, 1938, **6**, 620–629.
- 37 N. Ohno, W. Tokunaga and S. Mia, *Prediction of Pressure-Viscosity Coefficient Based on Sound Velocity of Lubricating Oils*, 2006.
- 38 T. Regueira, L. Lugo, O. Fandiño, E. R. López and J. Fernández, *Green Chemistry*, 2011, **13**, 1293–1302.
- 39 W. Żwirbla, A. Sikorska and B. B. Linde, *Journal of Molecular Structure*, 2005, **743**, 49 – 52.
- 40 P. Attri, P. M. Reddy and P. Venkatesu, *Indian Journal of Chemistry -Section A (IJC-A)*, 2010, **49A**, 736–742.
- 41 M. Dzida, E. Zorębski, M. Zorębski, M. Żarska, M. Geppert-Rybczyńska, M. Chorążewski, J. Jacquemin and I. Cibulka, *Chemical Reviews*, 2017, **117**, 3883–3929.
- 42 V. Syamala, P. Venkateswarlu, G. Prabhakar and K. Sivakumar, *Physics and Chemistry of Liquids*, 2006, **44**, 127–137.
- 43 Y. Lei, H. Li, H. Pan and S. Han, *The Journal of Physical Chemistry A*, 2003, **107**, 1574–1583.
- 44 C. Zhang, Z. Ren, L. Liu and Z. Yin, *Molecular Simulation*, 2013, **39**, 875–881.
- 45 K. Trachenko, *Phys. Rev. B*, 2008, **78**, 104201.
- 46 D. Bolmatov, V. V. Brazhkin and K. Trachenko, *Scientific Reports*, 2012, **2**, 421.
- 47 V. V. Brazhkin and K. Trachenko, *The Journal of Physical Chemistry B*, 2014, **118**, 11417–11427.
- 48 N. Anwar and Riyazuddeen, *Journal of Solution Chemistry*, 2016, **45**, 1077–1094.
- 49 Y. U. Paulechka, A. G. Kabo, A. V. Blokhin, G. J. Kabo and M. P. Shevelyova, *Journal of Chemical & Engineering Data*, 2010, **55**, 2719–2724.
- 50 Y. U. Paulechka, *Journal of Physical and Chemical Reference Data*, 2010, **39**, 033108.
- 51 E. Brini, C. J. Fennell, M. Fernandez-Serra, B. Hribar-Lee, M. Lukšič and K. A. Dill, *Chemical Reviews*, 2017, **117**, 12385–12414.
- 52 T. Murphy, L. M. Varela, G. B. Webber, G. G. Warr and R. Atkin, *The Journal of Physical Chemistry B*, 2014, **118**, 12017–12024.